A sensor for superoxide in aqueous and organic/aqueous media based on immobilized cytochrome *c* on binary self-assembled monolayers

Xueping Ji[a, b, *], Jujie Ren[b], Jiye Jin[b] and Toshio Nakamura[b]

[a]Department of Medical Chemistry, Hebei Medical University, Shijiazhuang 050017, China

[b]Department of Chemistry, Faculty of Science, Shinshu University, Matsumoto 390-8621, Japan

Abstract

A method for the electrochemical detection of superoxide radical was developed, based on cytochrome *c* (cyt *c*) immobilized on the binary self-assembled monolayers (SAMs) of thioctic acid (T-COOH) and thioctic amide (T-NH_2) on gold electrode. The sensor works by electrochemically detecting cyt *c* reduced by the superoxide radical generated by a xanthine-XOD system. The electrochemical properties of immobilized cyt *c* were investigated in aqueous buffer and in a mixture of aqueous and organic solvents. The interaction of superoxide radical with the modified electrode was characterized in phosphate buffer solution (PBS) and in the mixtures of both PBS and dimethyl sulfoxide (DMSO) and PBS and glycerol (Gly). The results showed that the sensors responded immediately to superoxide radical in PBS and gave a steady-state anodic current within 10 s during the generation of superoxide radical. In 40% DMSO and in 30% Gly solution, the current response reached a steady-state anodic current within 20 s. The sensor could also be used to estimate superoxide dismutase (SOD).

Keywords: Superoxide sensor; Self-assembled monolayers; Cytochrome *c*; Gold electrode; Organic solvents

1. Introduction

Superoxide radical belongs to the group of reactive oxygen species produced in biological respiration and metabolism, and it may damage organisms if it exceeds the level at which these organisms are able to protect themselves from its effects. Superoxide radical is believed to be closely implicated in a number of biological phenomena, such as aging ([Mannino et al., 1999], [Pinzino et al., 1999], [Hensley and Floyd, 2002] and [Youdim and Joseph, 2001]) and diseases (Hancock, 1997). The detection of superoxide radical is thus essential if we are to better understand the radical's role in degenerative processes and more accurately diagnose the diseases in which it is involved.

The quantitative detection of superoxide radical concentration in biological models is very difficult due to its fleeting existence and low concentration. Most techniques for the detection of superoxide radical use indirect spectroscopic methods (Fridovich, 1997), such as spectrophotometric measurement (Haseloff et al., 1991), chemiluminescence method (Reichl et al., 2001), and electron spin resonance spectroscopy (Harbour and Hair, 1978). However, these strategies are ex situ detection techniques with poor selectivity or sensitivity.

A new amperometric sensor technique has been developed to detect superoxide radical both in vitro and in vivo. It is based on a promotor-modified gold electrode on which cyt *c* is immobilized ([Lisdat et al., 1999] and [McNeil et al., 1995]). Superoxide radical reduces the immobilized cyt *c*, which can be immediately reoxidized by the electrode at a suitable potential.

This electrochemical strategy offers specific advantages, including the possibility of on-line measurement, minimum disturbance of chemical/enzymatic interventions, measurement in vivo, and low equipment cost.

Recently, single component COOH monolayers ([Lisdat et al., 1999] and [Scheller et al., 1999]) and mixed-monolayers of short alkanethiols (Gobi and Mizutani, 2000) with immobilized cyt *c* gold electrodes have been employed in the electrochemical detection of superoxide radical. However, amperometric sensors are limited both by the amount of cyt *c* immobilized in the SAMs and the rate of electron transfer between cyt *c* and electrode. Therefore, the development of a new sensor surface giving an increase in protein loading and a more efficient electron transfer is very important.

Recently, we have developed a new type of binary SAMs composed of thioctic acid (T-COOH) and thioctic amide (T-NH_2) to modify gold electrode (Ji et al., 2006). This binary SAMs is superior for attaching cyt *c*. T-COOH and T-NH_2, with disulfide-containing bases, have distinct advantages for gold electrode modification. The disulfide-containing base yields two gold-sulfur bonds and gives additional stability, compared with the single gold-sulfur bond formed by alkanethiols with gold surface. Furthermore, the components of the terminal groups of the SAMs composed

of T–COOH/T–NH_2, carboxyl and amino, match the residual groups (—NH_2 and —COOH) of protein, making the interaction between the SAMs and cyt *c* strong and the amount of adsorbed cyt *c* increase, due to the electrostatic interaction and steric effect between SAMs and cyt *c*.

The use of protein–based sensors has mostly been limited to studies in aqueous buffer. In order to broaden the range of applications, sensors have also been developed for use not only in aqueous buffer but also in mixtures of the aqueous and organic solvents of a system (Beissenhirtz et al., 2003).

In our study, a sensor based on the direct electron transfer of cyt *c* immobilized on binary SAMs was used to detect superoxide radical in PBS and in the mixtures of both PBS and dimethyl sulfoxide (DMSO) and PBS and glycerol (Gly). The effect of the mixtures of PBS and organic solvents on the electrochemical behavior of cyt *c* immobilized on T–COOH/T–NH_2 modified electrode was investigated in this study. The influence of hydrogen peroxide (H_2O_2) and uric acid on the sensor signal was also investigated. Additionally, the sensor was used to estimate of SOD activity.

2. Experimental

2.1. Materials, buffers, and mixture solutions

Superoxide dismutase (SOD), Dimethylsulfoxide (DMSO), potassium ferricyanide, xanthine (Xa) and hydrogen peroxide (H_2O_2, 30%) were purchased from Wako Pure Chemical, Co. Ltd., and used as received. Glycerol (Gly) and tetraethylammonium perchlorate (TEAP), a polarographic grade product, were purchased from Nacalai

Tesque, Inc. Xanthine oxidase (XOD) was provided by Sigma. Other chemicals were of analytical reagent grade. Horse heart cyt *c* and other materials were the same as those used in a previous study (Ji et al., 2006).

Phosphate buffer solutions (PBS) were also prepared by the same method described in the paper referred to above. Four mM PBS, pH 7.0, was used for the preparation of cyt *c* electrode, and 10 mM PBS, pH 7.0, served to record cyclic voltammograms, 10 mM PBS, containing 1.0 mM EDTA, pH 7.5, was used in the generation of superoxide radical. In order to ensure the high conductivity of all mixtures, TEAP was added to DMSO and Gly, leading to a final concentration of 30 mM. The mixture solutions were prepared freshly in the cell by adding the desired volume of organic solvents (containing 30 mM TEAP) to 10 mM PBS (pH 7.5).

2.2. Preparation of modified electrodes and electrochemical measurement

The gold disk electrodes were prepared and cyclic voltammetry was carried out in the same way as reported in the previous paper (Ji et al., 2006). All potential values given below are referenced to Ag/AgCl/3 M NaCl. The surface concentration (/⁻) of cyt *c* on the modified gold electrode can be calculated by the slope of the line. Amperometric measurements were taken using a potentiostat/galvanostat combined with an arbitrary function generator (HOKUTO DENKO) and an x–y recorder. The current–time data were recorded by applying a potential of +150 mV on a stirred cell.

3. Results and discussion

3.1. Electrochemistry of cyt *c* immobilized on binary SAMs

The electrochemical behavior of immobilized cyt *c* was investigated by cyclic voltammetry in our previous study (Ji et al., 2006). A pair of well-defined quasi-reversible redox peaks occurred. The formal potential, $E^{\circ\prime}$, taken as the average of E_{pc} and E_{pa}, was −0.032 V, with ΔE_p, the peak-to-peak potential separation of anodic and cathodic waves, 0.010 V at a scan rate of 40 mV s^{-1}, as shown in Fig. 1. The redox peak currents (the ratio of the anodic and cathodic peak currents was close to 1.0) were directly proportional to the potential scan rates at low scan rates.

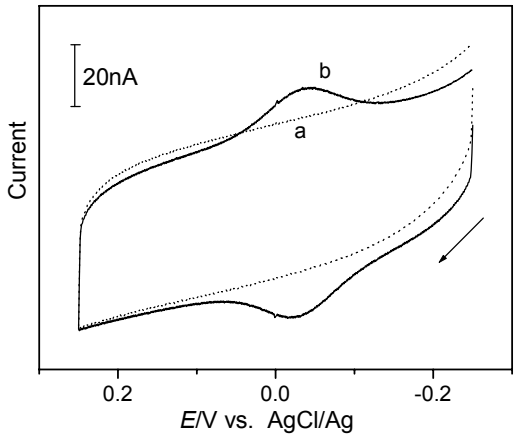

Fig. 1. Cyclic voltammograms of the cyt c/T-COOH/T-NH_2/Au electrode (T-COOH:T-NH_2=3:2 in adsorption solution) in 10 mM PBS (pH 7.0) before (a) and after (b) adsorption from the solutions of 0.05 mg mL^{-1} cyt c. Scan rate: 40 mV s^{-1}.

The surface concentration (Γ) and the heterogeneous electron transfer rate constant (k) of cyt *c* on the modified gold electrode were 9.2 × 10^{-12} mol cm^{-2} and 15.8 ± 0.6 s^{-1} at a ratio of T-COOH to T-NH_2 of 3:2.

The blockage of the binary monolayer of T–COOH and T–NH_2 modified electrode for potentially interfering substances was examined. Fig. 2 illustrates the efficient blockage of SAMs modified electrode surface for interfering substances. The bare Au electrode in hexacyanoferrate solution (1 mM $[Fe(CN)_6]^{3-}/[Fe(CN)_6]^{4-}$ in 0.1 M PBS, pH 7.5) showed a well–defined Faradaic response. In contrast, the cyclic voltammograms for electrodes prepared with T–COOH and T–NH_2 at a ratio of 3:2 showed effective blocking for this redox couple. This was attributed to the repulsing interaction of the negative charge on the SAMs to the negatively charged redox couple ($[Fe(CN)_6]^{3-}/[Fe(CN)_6]^{4-}$), indicating that the SAMs inhibited penetration of the ferricyanide and ferrocyanide redox species.

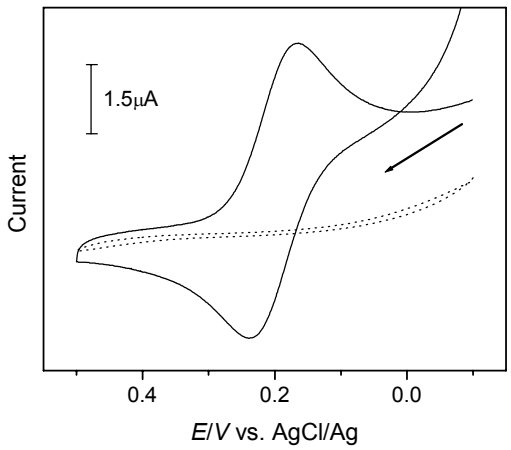

Fig. 2. Cyclic voltammograms of the bare Au electrode (solid line) and the T-COOH/T-NH_2/Au electrode (dotted line, T-COOH:T-NH_2=3:2 in adsorption solution) in 0.1 M PBS solution, pH 7.5, containing 1mM $[Fe(CN)_6]^{3-}/[Fe(CN)_6]^{4-}$. Scan rate: 20 mV s^{-1}.

3.2. Effect of organic solvents on the electrochemical behavior of cyt *c*

The electrochemical behavior of the cyt c/T–COOH/T–NH_2/Au electrode in mixtures of aqueous buffer and DMSO, acetonitrile (AN), *N*,*N*–dimethylformamide (DMF), *N*,*N*–dimethylaccetamide (DMA), and Gly was investigated. DMSO, AN, and DMF were selected due to the reversible electrochemistry of soluble cyt *c* in the resulting mixtures (Sivakolundu and Mabrouk, 2000). Furthermore, they are dipolar aprotic solvents, in which superoxide is quite stable (Che et al., 1996). 95% Gly sustained cyt *c* electrochemical activities on TiO_2 modified SnO_2 electrode ([Grealis and Magner, 2002] and [Grealis and Magner, 2003]).

Starting with 5% organic solvent, the volume percentage was increased until no cyt *c* redox peaks were observed. The peak currents (i_p) decreased as the volume percentage of organic solvents increased for all organic solvents. When the volume percentage of organic solvents exceeded 30%, no peak currents were observed for AN, DMA, or DMF. However, the highest possible contents of DMSO and Gly still sustaining cyt *c* electrochemical activities were 50% and 90%, respectively. Dependence of the peak currents of the cyt *c* electrode on the organic solvent contents is shown in Fig. 3A (only for DMSO and Gly). The i_p value decreased first slightly with increasing DMSO content. However, further increase in the proportion of DMSO resulted in a sharp decrease in i_p. In 40% DMSO, i_p was 25.5 nA, a decrease of 34% compared with that in the PBS (38.5 nA).

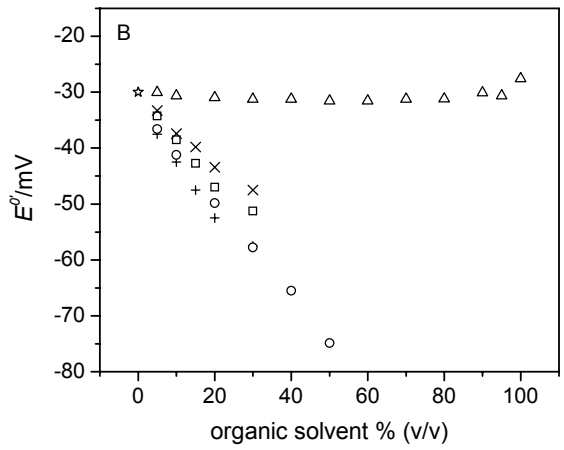

Fig. 3. Dependence of the peak currents (A) and formal potential (B) of the cyt c electrode on the organic solvent content. Scan rate: 200 mV s^{-1}, *vs.* Ag/AgCl/ 3 M NaCl. (A) Square: PBS, circles: DMSO, triangles: Gly. (B) Star: PBS, pluses: DMA, squares: AN, crosses: DMF, circles: DMSO, triangles: Gly.

In contrast to DMSO, i_p value decreased first sharply with increasing Gly content, then with further increase in the proportion of Gly, this decrease leveled off. In 30% and 60% Gly, i_p values are 21 nA and 13 nA, decreases of 46% and 67% compared with that in PBS (38.5 nA).

In the range of organic solvent concentrations we were interested in, the $E^{\circ\prime}$ value was found to decrease linearly with increasing concentrations of AN (= 35.9), DMF (= 36.7), DMA (= 37.8), and DMSO (= 46.5). However, for Gly (= 42.5), almost no obvious decrease in $E^{\circ\prime}$ was observed with increasing concentrations of Gly, as shown in Fig. 3B.

Some electrochemical parameters observed here for immobilized cyt *c* on COOH/NH_2 SAMs are in agreement with the behavior of cyt *c* immobilized on COOH/OH SAMs observed by Sivakolundu and Mabrouk (2000).

The linear decrease in $E^{\circ\prime}$ observed with increasing concentration of DMSO was similar to that in Beissenhirtz et al. (2003), in which cyt *c* was covalently immobilized on a COOH/OH modified electrode. The slope of the linear function was nearly identical, indicating that the different promoter layer produced had rather little effect on $E^{\circ\prime}$ shift in the same mixture.

The electrochemical behavior of cyt *c*, such as formal potential and anodic and cathodic currents, with increasing content of organic solvents was dependent on the permittivity of the mixtures. As the amount of organic solvents increased, the permittivity decreased, leading to an alteration in the microenvironment surrounding cyt *c*. One possible change is the rupture of the hydrogen bonding network, which may result in the structural conversion of cyt *c* on the electrode and may cause desorption of cyt *c* from the surface of the electrode, leading to the decreasing of peak current of cyt *c*. On the other hand, the permittivity decrease may also decrease the ionization degree of $\equiv$COOH and $\equiv NH_2$ in both of binary SAMs and cyt *c*. Cyt *c* is positively charged at pH 7.0 due to its isoelectric point of 10.4 (Barlow and Margoliash, 1966), so with increasing the content of organic solvents the positive charge of cyt *c* may decrease. According to complex compound theory, the decrease of the positive charge may let ferricyt *c* become more stable than ferrocyt *c*, so leading to a decrease of $E^{\circ\prime}$ of cyt *c*. However, permittivity is not the only factor influencing the electrochemical behavior of immobilized cyt *c*. For Gly, although its permittivity

(= 42.5) is smaller than that of DMSO, $E^{\circ\prime}$ was almost unchanged with increasing concentration of Gly. In these five organic solvents, Gly is different from the others. AN, DMA, DMF, and DMSO are aprotic solvents, but Gly is a protic solvent. It may have not produce obvious effect on the microenvironment of cyt *c*, resulting in no change in $E^{\circ\prime}$ with increasing content of Gly.

3.3. Interaction of superoxide with the cyt *c*/T–COOH/T–NH_2/Au electrode

3.3.1. Electrochemical response of superoxide radical

Cyclic voltammetric experiments were performed in the absence and presence of superoxide radical generated in situ by enzymatic reaction of XOD with xanthine in 10 mM PBS (pH 7.5), containing 0.1 mM EDTA, as shown in Fig. 4A.

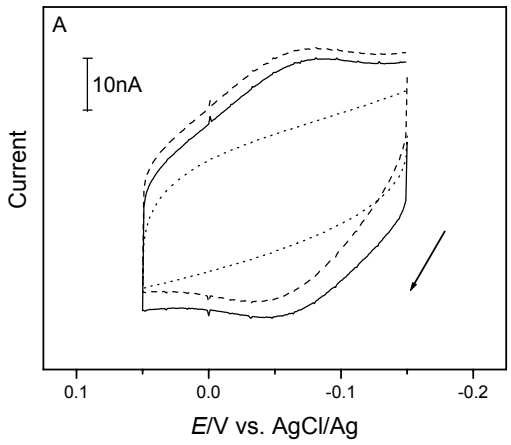

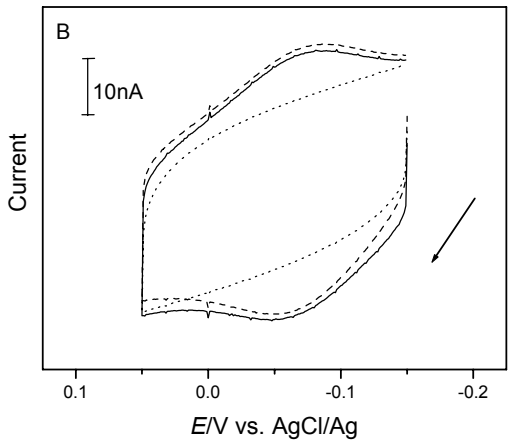

Fig. 4. Cyclic voltammograms at theT-COOH/T-NH_2/Au electrode in electrolyte solutions in the presence of 5 U ml^{-1} catalase and 200 μM xanthine after addition of XOD (dotted line), and at the cyt c/ T-COOH/T-NH_2/Au electrode before (dashed line) and after (solid line) addition of XOD to 249 $mUml^{-1}$. (A) in 10 mM PBS (pH=7.5, containing 1 mM EDTA); (B) in 60% PBS+40%DMSO (containing 30 mM TEAP). Scan rate: 20 mV s^{-1}.

No redox currents were observed at a modified gold electrode (cyt *c* free) during the generation of the superoxide radical, as shown in Fig. 4(A, a), which demonstrates that the superoxide radical cannot be directly oxidized at the modified gold electrode (cyt *c* free). This can be attributed to the blocking of SAMs on the surface of the gold (vide supra and Fig. 2). In contrast, cyclic voltammograms for immobilized cyt *c* electrode showed an increase in oxidation current with a decrease in reduction current during the generation of the superoxide radical (Fig. 4(A, c)), compared with the case in which no superoxide radical was generated (Fig. 4(A, b)). The electrocatalytic behavior of cyt

c in response to the oxidation of superoxide radical indicates that the superoxide radical is oxidized electrocatalytically by cyt *c* and not at the gold electrode.

Cyclic voltammograms for the immobilized cyt *c* electrode in the mixture of 60% PBS and 40% DMSO also showed an increase in oxidation current with a decrease in reduction current during the generation of superoxide radical, as shown in Fig. 4(B, c), compared with the case in which no superoxide radical was generated (Fig. 4(B, b)), but the changes of peak currents were smaller than in PBS.

3.3.2. Amperometric response of superoxide radical

The amperometric response of superoxide radical was investigated at the applied potential of +150 mV both in PBS and in the mixture of PBS and organic solvent.

Typical response of cyt *c* immobilized electrode on the addition of 160 mU mL^{-1} XOD to the 10 mM PBS in the presence of 160 μM xanthine and 5 U mL^{-1} catalase is shown in Fig. 5a. A stable background current was obtained before the addition of XOD. On the addition of XOD, the current immediately increased anodically and reached a plateau within 10 s. The magnitude of the oxidation current was 3.3 nA. The responses of cyt *c*–immobilized electrode in the mixture solutions of PBS and DMSO or Gly are also shown in Fig. 5. On the addition of XOD to the mixture of 60% 10 mM PBS and 40% DMSO (Fig. 5b), the current response became a little slower than in PBS, and reached a plateau within 20 s. The magnitude of the oxidation current was 2.3 nA, which was smaller than in PBS.

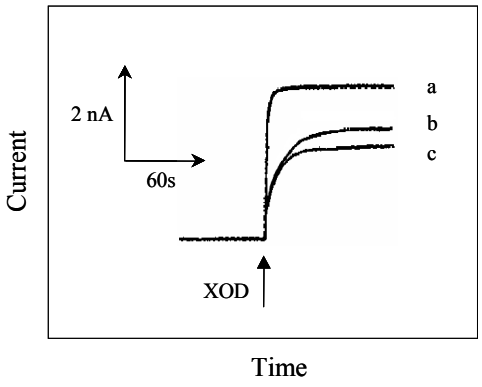

Fig. 5. Amperometric response of the cyt c/T-COOH/T-NH_2/Au recorded at +150 mV on the addition of 160 mU mL^{-1} XOD to electrolyte solutions in the presence of 5 U mL^{-1} catalase and 160 μM xanthine. (a) PBS; (b) 60% PBS+40% DMSO (containing 30 mM TEAP); (c) 70% PBS and 30% Gly (containing 30 mM TEAP).

On the addition of XOD to the mixture of 70% 10 mM PBS and 30% Gly (Fig. 5c), the oxidation current response also became slower than in PBS, and within 20 s reached a stable current of 2.0 nA.

As the concentration of Gly increased to 60% in the mixture solution, the oxidation current response became slower than in 30% Gly. A 1.6 nA oxidation current was obtained.

The superoxide radical generated by xanthine–XOD can undergo spontaneous dismutation into O_2 and H_2O_2 in solution. The counterbalance between the generation

and disproportionation of the superoxide radical will result in a constant equilibrium concentration of the superoxide radical in solution.

The superoxide radical generated by the xanthine–XOD system reduced Cyt *c* immobilized on the modified gold electrode, and then the reduced cyt *c* was oxidized electrochemically.

The diffusion velocity of superoxide radical in DMSO or Gly is slower than in aqueous due to the greater viscosity of DMSO (1.99 cp) and Gly (934 cp) compared with water (0.89 cp) (Izutsu, 2002), which results in the current response in 40% DMSO or 30% Gly becoming slower than in the PBS. Although the current response in 40% DMSO or 30% Gly is slower than in the PBS, it is fast enough to make it possible to detect the superoxide radical.

The observation of a lower current response for superoxide radical in mixtures than in the PBS can be explained in three ways. Firstly, although cyt *c* electrochemical activity can be sustained up to 40% DMSO and 80% Gly (Fig. 3A), the peak currents of the cyclic voltammograms in 40% DMSO and 30% and 60% Gly are about 66%, 54%, and 33% of that in PBS, respectively. The decrease in the electrochemical activity of cyt *c* adsorbed on the surface of the electrode results in lower oxidation of superoxide radical. Secondly, the activity of XOD itself decreases in the mixtures of aqueous buffer and organic solvents, which also leads to a decrease in the current response of superoxide radical (Beissenhirtz et al., 2003). Finally, lower oxidation of superoxide radical arises from the decrease of catalytic activity between superoxide and cyt *c* in the mixtures.

Although, the magnitudes of oxidation currents in 40% DMSO and 30% Gly are lower than those in the PBS, they are sufficient to enable detection of the superoxide radical in solution. However, when the concentration of Gly increased to 60%, detection became more difficult due to the lower oxidation current.

3.3.3. Interference of H_2O_2 and uric acid in the detection of the superoxide

During the generation of superoxide radical, H_2O_2 and uric acid are coproduced in the electrolyte solution. The effects of both H_2O_2 and uric acid were investigated because the experiment made use of an enzymatic reaction, which leads to the formation of these redox-active substances.

Additions of uric acid to the solution were investigated in the absence of superoxide radical at an applied potential of +150 mV. The sensor electrode gave no response to this reducing acid up to concentrations of 3 mM either in PBS or in the mixture of PBS and 40% DMSO or PBS and 30% Gly.

The cyt *c*-immobilized electrode can exhibit pseudo-peroxidase activity. For the cyt *c*/T-COOH/T-NH_2/Au electrode, this was particularly pronounced at *E*-values lower than +100 mV. At +150 mV, a reduction current in the electrode was still observed in the absence of superoxide radical. On addition of H_2O_2 at concentrations of less than 100 μM, the reduction current resulting from the oxidation of cyt *c* by H_2O_2 was low and did not disturb the sensor performance. For concentrations of H_2O_2 higher than 100 μM, the reduction current was already visible both in PBS and in the mixtures. (Lisdat et al., 1999). The effect of 1 mM H_2O_2 in PBS or in the mixture of PBS and 40%

DMSO or PBS and 30% Gly was suppressed by adding 5 U mL^{-1} of catalase to the solution.

3.3.4. Amperometric detection of superoxide radical

The sensors were examined for the detection of superoxide radical in PBS or in the mixtures. Calibration for superoxide measurement requires that the spontaneous dismutation of the superoxide be taken into account. The counterbalance between superoxide generation (1) and its dismutation (2) will result in a steady-state sensor signal. The signal level is proportional to the square root of XOD activity (McCord and Fridovich, 1968).

$$\text{Xanthine } (O_2) + H_2O \xrightarrow{\text{XOD, } k_1} \text{urate} + O_2^{\bullet -} \qquad (1)$$

$$2O_2^{\bullet -} + 2H^+ \xrightarrow{k_2} O_2 + H_2O_2 \qquad (2)$$

At steady state,

$$v_1 = 2v_2 \qquad (3)$$

$$k_1[\text{XOD}] = 2k_2[O_2^{\bullet -}]^2 \qquad (4)$$

$$[O_2^{\bullet -}] = \sqrt{k_1/(2k_2) \bullet [\text{XOD}]} \qquad (5)$$

At steady state,

The k_1 value was 1 s^{-1} for the enzyme under air saturation of the solutions (McCord and Fridovich, 1968), and the k_2 value for the spontaneous dismutation of $O_2^{\bullet -}$ is given as 2.3 × 10^{-5} M^{-1} s^{-1} at pH 7.5 (Behar et al., 1970).

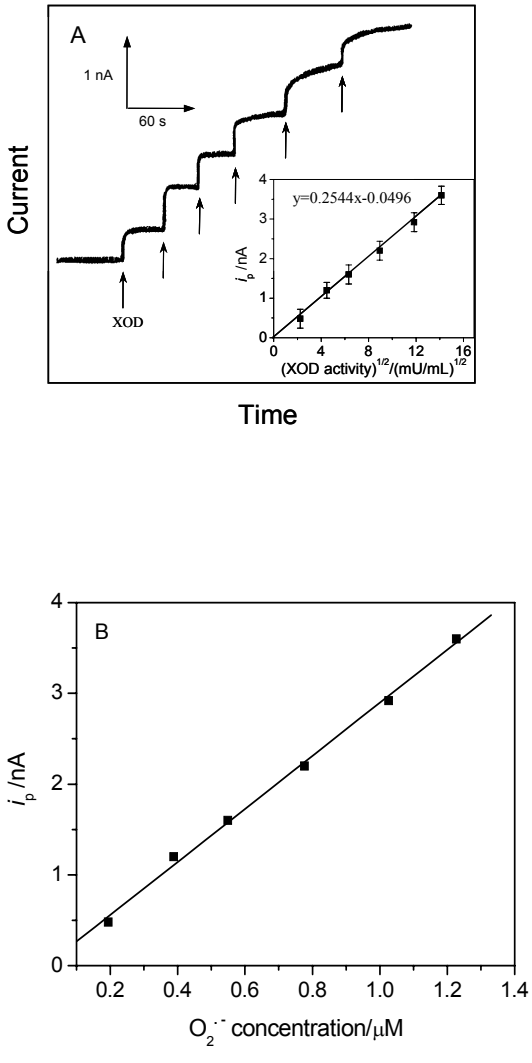

Fig. 6. (A) Response of the cyt c/T-COOH/T-NH_2/Au recorded at +150 mV on successive addition of 5, 15, 20, 40, 60, and 60 mU mL^{-1} XOD to PBS in the presence of 5 U mL^{-1} catalase and 160 μM xanthine. Inset: relationship between steady-state current and the square root of XOD activity; (B) Dependence of the sensor signal in PBS on the theoretically estimated $O_2^{\bullet-}$ concentration.

Fig. 6A showed the response of the sensor to XOD activity in PBS. As shown in Fig. 6(A, inset), the sensor signal was proportional to the square root of XOD from 5 to 200 mU mL^{-1} XOD. The results indicate that the sensor is fast enough to follow the actual concentration of superoxide in in vivo analysis. Fig. 6B shows the dependence of the sensor signal on the theoretically estimated $O_2{\cdot}^-$ concentration according to Eq. (5). The linear response to $O_2{\cdot}^-$ concentration is up to 1.23 μM. From the slope of 2.92 nA μM^{-1}, a sensitivity of 9.3 × 10^2 A m^{-2} M^{-1} was obtained. Compared with the sensitivities reported for a mixed long-chain thiol (Ge and Lisdat, 2002) and a single-component short-chain thiol modified electrode (Tammeveski et al., 1998), the results we obtained using the binary SAMs of T-COOH and T-NH_2 modified electrode were better by factors of 3.3 and 16.6, respectively.

The response of the sensor to XOD activity in 40% DMSO was proportional to the square root of XOD from 1 to 8 mU mL^{-1} XOD. The linear regression equation is $y = 0.3001x - 0.01756$ and the slope, 0.3001, is higher than in PBS (0.2544). It can be explained as follows. Superoxide radical can exist in DMSO very stably, but in aqueous solution it spontaneously and immediately dismutates into O_2 and H_2O_2. So, we would expect superoxide radical to exist for a longer period in 40% DMSO than in aqueous buffer, which would lead to an increase in current response. Furthermore, the sensor response to the substrate concentration of superoxide was also investigated.

The apparent Michaelis-Menten constant, $K_{m,}$ a reflection of enzymatic affinity, can be calculated according to the Lineweaver-Burk equation ([Mell and Maloy, 1975], [Shu and Wilson, 1976] and [Kamin and Wilson, 1980]).

$$i^{-1} = i_{max}^{-1} K_{m,app} [S]^{-1} + i_{max}^{-1} \quad (6)$$

where [S] is the concentration of substrate.

The apparent constant K_m for the reaction of XOD with xanthine was calculated to be 1.75 ± 0.08 μM, which is similar to the value given in the literature (Lisdat et al., 1999). The K_m values for enzymatic reaction in 40% DMSO at the cyt *c*–immobilized electrode were calculated to be 1.40 ± 0.10 μM, which is slightly lower than in pure buffer.

3.3.5. Estimation of superoxide dismutase enzyme

From the results above, we know that the cyt *c*–immobilized electrodes respond immediately to the superoxide radical under the conditions of the experiment and produce a steady–state oxidation current during the enzymatic generation of superoxide radical. It is well known that SOD is a selective scavenger of superoxide radical. On the addition of SOD to the system of superoxide radical generation, the superoxide radical will be dismutated into H_2O_2 and O_2 immediately, resulting in a decrease in oxidation current. So a sensor based on a cyt *c*–immobilized electrode could also be used to detect SOD. The amperometric responses of the cyt *c*–immobilized electrode to SOD during the enzymatic generation of superoxide radical were estimated in PBS and in the mixtures of both PBS and DMSO and PBS and Gly. On the addition of 200 mU mL^{-1} XOD and 30 U mL^{-1} SOD to 10 mM PBS in the presence of 5 U mL^{-1} catalase and 200 μM xanthine, the steady–state oxidation current of the superoxide radical decreased immediately and attained a new steady

state within 10 s. The magnitude of decrease in the oxidation current was 3.2 nA (decreased by 64%, on addition of SOD).

The steady-state oxidation current of the superoxide radical decreased immediately on addition of SOD to a mixture solution of 60% 10 mM PBS and 40% DMSO and reached a new steady-state within 20 s. The magnitude of decrease in the oxidation current was 1.3 nA (a decrease of 30%). On the addition of SOD to the mixture solution of 70% 10 mM PBS and 30% Gly the steady-state oxidation current decreased by 0.9 nA within 20 s (a decrease of 43%). However, as the concentration of Gly increased to 60% in the mixture solution, almost no decrease in the oxidation current of superoxide radical was observed on the addition of SOD. In other words, SOD is almost unable to scavenge superoxide radical in 60% Gly solution.

Our results show that SOD scavenges superoxide radical most effectively in the PBS. In the 40% DMSO or 30% Gly solution SOD can also work effectively to scavenging superoxide radical, but it becomes weaker than in the PBS.

4. Conclusion

An electrochemical sensor for the detection of superoxide radical in PBS and in the mixtures of PBS and organic solvents was developed in this study. The sensor is based on the detection of superoxide concentration by a cyt *c*–immobilized gold electrode. A binary SAMs of T-COOH and T-NH_2 was used for cyt *c* immobilization of the electrode, and this worked to protect the electrode surface from potential interfering species in the solution.

These investigations in combination with the stability of superoxide radical in dipolar aprotic solvents (DMSO, AN, DMF, and DMA) allowed the identification of suitable aqueous mixture mediums of 40% DMSO or 30% Gly. The sensor responsed quickly to $O_2{\cdot}^-$ in PBS and in the mixtures of 60% PBS and 40% DMSO, and the sensitivity of the sensor in 40% DMSO was higher than in PBS when the concentration of XOD is less than 8 mU mL^{-1}. The sensor could also be used to estimate SOD.

The proposed method would provide on-line detection with relatively simple equipment, low costs, and high sensitivity, compared to chromatographic methods.

References

Barlow and Margoliash, 1966 G.H. Barlow and E. Margoliash, *J. Biol. Chem.* 241 (1966), pp. 1473-1477. View Record in Scopus | Cited By in Scopus (21)

Behar et al., 1970 D. Behar, G. Czapski, J. Rabani, L.M. Dorfman and H.A. Schwarz, *J. Phys. Chem.* 74 (1970), pp. 3209-3213. Full Text via CrossRef | View Record in Scopus | Cited By in Scopus (93)

Beissenhirtz et al., 2003 M. Beissenhirtz, F. Scheller and F. Lisdat, *Electroanalysis* 15 (2003), pp. 1425-1435. Full Text via CrossRef | View Record in Scopus | Cited By in Scopus (10)

Che et al., 1996 Y. Che, M. Tsushima, F. Matsumoto, T. Okajima, K. Tokuda and T. Ohsaka, *J. Phys. Chem.* 100 (1996), pp. 20134-20137. Full Text via CrossRef | View Record in Scopus | Cited By in Scopus (18)

Fridovich, 1997 I. Fridovich, *J. Biol. Chem.* 272 (1997), pp. 18515–18517. Full Text via CrossRef | View Record in Scopus | Cited By in Scopus (375)

Ge and Lisdat, 2002 B. Ge and F. Lisdat, *Anal. Chim. Acta* 454 (2002), pp. 53–64. SummaryPlus | Full Text + Links | PDF (166 K) | View Record in Scopus | Cited By in Scopus (50)

Gobi and Mizutani, 2000 K.V. Gobi and F. Mizutani, *J. Electroanal. Chem.* 484 (2000), pp. 172–181. SummaryPlus | Full Text + Links | PDF (163 K) | View Record in Scopus | Cited By in Scopus (44)

Grealis and Magner, 2002 C. Grealis and E. Magner, *Chem. Commun.* 8 (2002), pp. 816–817. Full Text via CrossRef | View Record in Scopus | Cited By in Scopus (3)

Grealis and Magner, 2003 C. Grealis and E. Magner, *Langmuir* 19 (2003), pp. 1282–1286. Full Text via CrossRef | View Record in Scopus | Cited By in Scopus (13)

Hancock, 1997 J.T. Hancock, *Br. J. Biomed. Sci.* 54 (1997), pp. 38–46. View Record in Scopus | Cited By in Scopus (45)

Harbour and Hair, 1978 J.R. Harbour and M.L. Hair, *J. Phys. Chem.* 82 (1978), pp. 1397–1399. Full Text via CrossRef | View Record in Scopus | Cited By in Scopus (67)

Haseloff et al., 1991 R.F. Haseloff, B. Ebert and G.G. Wischnewsky, *Anal. Chim. Acta* 243 (1991), pp. 221–225. Abstract | View Record in Scopus | Cited By in Scopus (2)

Hensley and Floyd, 2002 K. Hensley and R.A. Floyd, *Arch. Biochem. Biophys.* 397 (2002), pp. 377–383. Abstract | Abstract + References | PDF (89 K) | View Record in Scopus | Cited By in Scopus (75)

Izutsu, 2002 K. Izutsu, Electrochemistry in Nonaqueous Solutions, WILEY–VCH, Germany (2002) p. 5.

Ji et al., 2006 X. Ji, B. Jin, J. Jin and T. Nakamura, *J. Electroanal. Chem.* 590 (2006), pp. 173–180. SummaryPlus | Full Text + Links | PDF (260 K) | View Record in Scopus | Cited By in Scopus (3)

Kamin and Wilson, 1980 R.A. Kamin and G.S. Wilson, *Anal. Chem.* 52 (1980), pp. 1198–1205. Full Text via CrossRef | View Record in Scopus | Cited By in Scopus (236)

Lisdat et al., 1999 F. Lisdat, B. Ge, E. Ehrentreich-Forster, R. Reszka and F. Scheller, *Anal. Chem.* 71 (1999), pp. 1359–1365. Full Text via CrossRef | View Record in Scopus | Cited By in Scopus (53)

Mannino et al., 1999 S. Mannino, S. Buratti, M.S. Cosio and N. Pellegrini, *Analyst* 124 (1999), pp. 1115–1118. Full Text via CrossRef | View Record in Scopus | Cited By in Scopus (18)

McNeil et al., 1995 C.J. McNeil, D. Athey and W.O. Ho, *Biosens. Bioelectron.* 10 (1995), pp. 75–83. Abstract | View Record in Scopus | Cited By in Scopus (60)

Mell and Maloy, 1975 L.D. Mell and J.T. Maloy, *Anal. Chem.* 47 (1975), pp. 299–307. Full Text via CrossRef | View Record in Scopus | Cited By in Scopus (71)

McCord and Fridovich, 1968 J.M. McCord and I. Fridovich, *J. Biol. Chem.* 243 (1968), pp. 5753–5760. View Record in Scopus | Cited By in Scopus (304)

Pinzino et al., 1999 C. Pinzino, A. Capocchi, L. Galleschi, F. Saviozzi, B. Nanni and M. Zandomeneghi, *J. Agric. Food Chem.* 47 (1999), pp. 1333–1339. Full Text via CrossRef | View Record in Scopus | Cited By in Scopus (30)

Reichl et al., 2001 S. Reichl, A. Vocks, M. Petkovic, J. Schiller and J. Arnhold, *Free Radical Res.* 35 (2001), pp. 723–733. Full Text via CrossRef | View Record in Scopus | Cited By in Scopus (5)

Scheller et al., 1999 W. Scheller, W. Jin, E. Ehrentreich-Forster, B. Ge, F. Lisdat, R. Buttemeier, U. Wollenberger and F.W. Scheller, *Electroanalysis* 11 (1999), pp. 703–706. Full Text via CrossRef | View Record in Scopus | Cited By in Scopus (35)

Shu and Wilson, 1976 F.R. Shu and G.S. Wilson, *Anal. Chem.* 48 (1976), pp. 1679–1686. Full Text via CrossRef | View Record in Scopus | Cited By in Scopus (69)

Sivakolundu and Mabrouk, 2000 S.G. Sivakolundu and P.A. Mabrouk, *J. Am. Chem. Soc.* 122 (2000), pp. 1513–1521. Full Text via CrossRef | View Record in Scopus | Cited By in Scopus (40)

Tammeveski et al., 1998 K. Tammeveski, T.T. Tenno, A.A. Mashirin, E.W. Hillhouse, P. Manning and C.J. McNeil, *Free Radical. Biol. Med.* 25 (1998), pp. 973–978. SummaryPlus | Full Text + Links | PDF (94 K) | View Record in Scopus | Cited By in Scopus (31)

Youdim and Joseph, 2001 K.A. Youdim and J.A. Joseph, *Free Radical Biol. Med.* 30 (2001), pp. 583–594. SummaryPlus | Full Text + Links | PDF (122 K) | View Record in Scopus | Cited By in Scopus (108)